

Minimum-Delay Routing for Integrated Aeronautical *Ad Hoc* Networks Relying on Passenger-Planes in the North-Atlantic Region

Jingjing Cui, Dong Liu, Jiankang Zhang, Halil Yetgin, Soon Xin Ng and Lajos Hanzo

Abstract

Relying on multi-hop communication techniques, aeronautical *ad hoc* networks (AANETs) seamlessly integrate ground base stations (BSs) and satellites into aircraft communications for enhancing the on-demand connectivity of planes in the air. In this integrated AANET context we investigate the shortest-path routing problem with the objective of minimizing the total delay of the in-flight connection from the ground BS subject to certain minimum-rate constraints for all selected links in support of low-latency and high-speed services. Inspired by the best-first search and priority queue concepts, we model the problem formulated by a weighted digraph and find the optimal route based on the shortest-path algorithm. Our simulation results demonstrate that aircraft-aided multi-hop communications are capable of reducing the total delay of satellite communications, when relying on real historical flight data.

I. INTRODUCTION

With the proliferation of Internet services and applications, it is desirable to provide high-speed broadband access during flights above the clouds. As mentioned in Airbus' Global Market Forecast (GMF) [1], passenger traffic growth would increase by about 50% by the year 2038 and air traffic as a whole will grow at 4.3% annually over the next 20 years. This forecast further inspires the wide roll-out of in-flight Internet access in aeronautical systems. However, since aircraft fly at a high speed, it is challenging to integrate conventional terrestrial communication solutions into aeronautical systems.

Existing aircraft connectivity solutions can be broadly categorized into two classes [2], [3]: satellite to aircraft communication (S2AC) and direct aircraft to ground communication (DA2GC). At the time of writing in-flight connectivity of aircraft mainly depends on satellites. In particular, often geostationary Earth orbit (GEO) satellites are used for providing on-board connectivity for aircraft as a benefit of their near-global coverage, supporting longer-lasting connections than DA2GC and aircraft-to-aircraft communication (A2AC) without the need for handovers between GEO satellites. For example, GoGo has more than 1,000 aircraft that are equipped with in-flight satellite connectivity, relying on the Gogo 2Ku system, for improving the passengers' on-board Wi-Fi experience [4]. However, the large coverage area

of GEO satellites comes at the cost of high latency as well as substantial power loss. In particular, GEO satellites are at a distance of 35,768km, hence they suffer from a propagation delay of approximately 120 ms one-way delay from the ground to the satellite.

To circumvent the shortcomings of S2AC, DA2GC provides an alternative for providing low-latency, high-rate transmissions to aircraft [2]. The European Aviation Network (EAN) has been designed to deliver up to 75 Mbps per cell by combining an S-band satellite and the 4G LTE mobile terrestrial network [5]. However, the coverage area of DA2GC is limited, since the ground BSs can only be deployed on dry land, while about 2/3 of the earth's surface is covered by water. Furthermore, no ground BSs are available in remote airspaces, such as the polar regions, deserts, dense forests, etc. In this context, aeronautical *ad hoc* networking constitutes a promising technique of extending the DA2GC by enabling aircraft in the sky to act as relays for aiding data transmission. In [6], the effects of both large-scale fading and small-scale fading on DA2GC channels were demonstrated in the C-band. As a further advance, a resource management scheme designed for satellite based terrestrial networks was investigated in [7].

A key issue of routing in integrated AANETs is the link selection from the set of D2AC, S2AC and A2AC channels across the routes, whilst meeting the specific application-oriented performance. In this paper, we concentrate on a special class of routing problems – namely the shortest-path routing of integrated AANETs, which is synonymous with minimizing the total service delay subject to per-connection quality of service (QoS) constraints. The shortest-path routing problem formulated can be solved over the associated weighted digraph by invoking the shortest path algorithm based on the idea of Dijkstra's algorithm [8], which is capable of delivering the optimal solution. We characterize our proposed algorithm by harnessing three real flight datasets based on flights over the North-Atlantic oceanic area. In particular, our results reveal that the aircraft can be connected to the ground BS through AANETs between London Heathrow (LHR) Airport and New York's John F Kennedy (JFK) Airport. Furthermore, both our simulations and real flight-data driven results demonstrate that the A2AC links are capable of extending the DA2GC coverage with the aid of low-delay transmission.

II. SYSTEM MODEL

A. Preliminaries of Pareto-optimal solutions

We consider a ground-air-space integrated AANET comprising the ground layer, the aerial layer and the space layer of Fig. 1, where aircraft can be connected to certain ground BSs either via direct communication or by multi-hop communication techniques. In particular, the aircraft can build communication links with other aircraft, ground BSs and satellites via A2AC, DA2GC and S2AC techniques, respectively, in order to improve the on-board Internet experience of aircraft passengers. We assume that the integrated

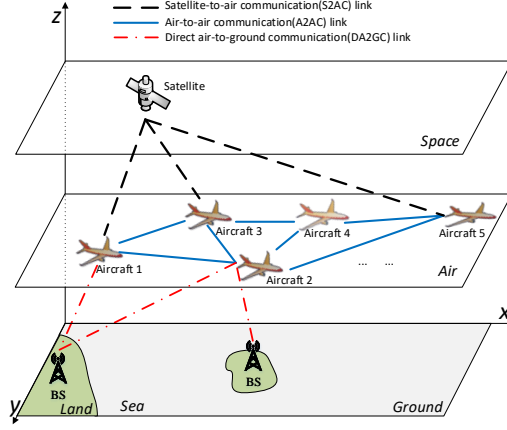


Fig. 1. Aircraft communication system by integrating ground and space communications.

AANET considered is composed of N_1 aircraft, N_2 ground BS and N_3 satellites, where an example of the system model is illustrated in Fig. 1. Furthermore, given the mobility of aircraft during its flight its location changes rapidly. For clarity, we denote the entities in the system encompassing aircraft, ground BSs and satellites as a set of nodes $\mathcal{N} = \mathcal{N}_1 \cup \mathcal{N}_2 \cup \mathcal{N}_3$ with $N = |\mathcal{N}|$, where $\mathcal{N}_1 = \{1, \dots, N_1\}$, $\mathcal{N}_2 = \{1, \dots, N_2\}$ and $\mathcal{N}_3 = \{1, \dots, N_3\}$. We assume that the integrated AANET is operated in half-duplex mode as in [9] and the messages from different ground BSs are transmitted on different subchannels resulting in no inter-link interference, representing an interference-free scenario.

Since aircraft typically fly 10km above the ground level, they benefit from negligible scatterers and shadowing effects. Hence we assume that the communication links in the AANET have LoS propagation [10]–[12], where the path-loss between node i and node j , $i, j \in \mathcal{N}$, can be expressed as

$$h_{i,j} = \left(\frac{c}{4\pi d_{i,j} f_c} \right)^\alpha, \quad (1)$$

where f_c is the carrier frequency and $c = 3 \times 10^8$ m/s is the speed of light. Furthermore, $d_{i,j}$ is the distance between node i as well as node j and α is the path-loss exponent.

B. Delay Model

In this paper, the delay model relies on the sum of the transmission and propagation delays of the individual connections. Moreover, we assume that the decode-and-forward (DF) relaying delay at each intermediate nodes is $D_{df} = 20$ ms.

Let us consider a communication link, where the message is sent from aircraft i to aircraft j . Hence the signal-to-noise ratio (SNR) at the receiver of aircraft j can be expressed as

$$\phi_{i,j} = \frac{P_i G_i^t G_j^r h_{i,j}}{\sigma^2}, \quad (2)$$

where σ^2 denotes the noise power. Furthermore, G_i^t and G_j^r are the transmit antenna gain and the receive antenna gain, respectively. Therefore, the data rate in the link spanning from node i to node j can be expressed as

$$C_{i,j} = B \log_2 \left(1 + \phi_{i,j} \right), \quad (3)$$

where B is the bandwidth allocated to the link. Correspondingly, given the size L of the data file to be transmitted in bits, the file-transfer delay between node i and node j can be calculated as

$$D_{i,j}^{tr} = \frac{L}{C_{i,j}}. \quad (4)$$

The propagation delay is the time it takes for the signal to travel at the speed of light through the communication link from a node to the next one, which is given by

$$D_{i,j}^{pr} = \frac{d_{i,j}}{c}, \quad (5)$$

where $D_{i,j}^{pr} = D_{j,i}^{pr}$. As a result, the total delay from node i to node j can be expressed as

$$D_{i,j} = \begin{cases} D_{i,j}^{tr} + D_{i,j}^{pr}, & \text{if } j \text{ is the target aircraft,} \\ D_{i,j}^{tr} + D_{i,j}^{pr} + D_{df}, & \text{otherwise.} \end{cases} \quad (6)$$

III. PROBLEM FORMULATION

Due to the curvature of the Earth, the maximum direct propagation distance between two aircraft is limited. Hence in addition to the QoS constraints, the communication between two nodes is also restricted by the radio-horizon, denoted as d_{vis} , which is relying on the height of the two nodes.

Our objective is to minimize the total delay of the links selected for transmission by appropriately selecting the routes between the source BS on the ground and the destination aircraft, which can be expressed as

$$\min_{x_{i,j} \in \mathcal{X}} \sum_{i \in \mathcal{N}} \sum_{j \neq i, j \in \mathcal{N}} D_{i,j} x_{i,j} \quad (7a)$$

$$\text{s.t. } x_{i,j} \phi_{i,j} \geq \phi_0, \quad i \text{ is not the target aircraft,} \quad (7b)$$

$$d_{i,j} \leq d_{vis}, \quad (7c)$$

$$\sum_{\substack{j \neq i \\ j \in \mathcal{N}}} x_{i,j} - \sum_{\substack{j \neq i \\ j \in \mathcal{N}}} x_{j,i} = \begin{cases} 1, & \text{if } i = s, \\ -1, & \text{if } i = d, \\ 0, & \text{otherwise,} \end{cases} \quad (7d)$$

$$\sum_{j \neq i, j \in \mathcal{N}} x_{i,j} \begin{cases} \leq 1, & \text{if } i \neq d, \\ = 0, & \text{if } i = d, \end{cases} \quad (7e)$$

$$\forall i, j \in \mathcal{N}, i \neq j, \quad (7f)$$

where s and d denotes the source and the destination, respectively. $x_{i,j}$ is the link indicator function used, where we have $x_{i,j} = 1$ if link (i, j) is on the optimal route; Otherwise $x_{i,j} = 0$. Furthermore, ϕ_0 is a predefined SNR threshold to be exceeded for guaranteeing the received signal quality, while the constraints in (7b) and (7c) ensure that a communication link spanning from node i to node j exists. Finally, constraints in (7d) and (7e) ensure that the solution found from the problem formulated does indeed represent a legitimate path spanning from the ground BSs to the target aircraft.

IV. SOLUTIONS FOR FINDING OPTIMAL ROUTES

As discussed in Section III, the delay minimization problem considered in this paper is an optimal route finding problem between the source node and the destination, which can be transformed into the optimal route-finding problem on a weighted digraph. Correspondingly, we first generate a weighted digraph based on the available network information. The initialization process is given in **Algorithm 1**, in which a weighted digraph $\mathcal{G}(\mathcal{V}, \mathcal{E})$ is constructed based on the system information and the constraints of (7b) as well as (7c), where \mathcal{V} and \mathcal{E} represent the set of the nodes and the edges, respectively. Note that the initialization process in **Algorithm 1** is capable of reducing the size of the weighted digraph generated by removing the redundant edges and nodes by considering the constraints in (7b) and the curvature of the earth in (7c).

Algorithm 1: Generated a weighted digraph based on AANETs

Input : The dataset for the number and the locations of aircraft, ground BSs and Satellites.

Output: Generated weighted digraph of ANETs

Init. : SNR threshold: ϕ_0 ; Values of system parameters: G^t , G^r , f_c and B ;

repeat

 For $i \in \mathcal{N}$, calculate the received SNR at every other node j from node i using (2) denoted as

$\phi_i = \{\phi_{i,j}, j \neq i \text{ and } j \in \mathcal{N}\};$

while $j \in \mathcal{N}$ and $j \neq i$ **do**

if $\phi_{i,j} \geq \phi_0$ and node j is visible to node i **then**

 Calculate the delay based on (6) as the weight of the edge $e_{i,j}$;

 Add edge $e_{i,j}$ and its weight $D_{i,j}$ into the graph \mathcal{G} ;

until all nodes are visited;

There are a number of approaches for finding the optimal route from the source to the destination such as Dijkstra's algorithm, dynamic programming as well as genetic algorithms. In this paper, we employ the

best-first search strategy (also called priority-first search) of Dijkstra's algorithm for finding the optimal route of the problem in (7), which is summarized in **Algorithm 2**.

Explicitly, the ground BS and the target aircraft are defined to be the source and the destination node, respectively. The total delay between any two nodes is treated as the 'cost' of the link. In addition, the priority queue structure is used for storing the candidate nodes as well as the correlated cost information during the search process. The procedure of **Algorithm 2** starts by introducing a set $\psi = \{\psi_0, \dots, \psi_N\}$ for storing the objective function (OF) values from the source node s to each of the other nodes during the search process. In ψ , all elements ψ_v , $v \in \mathcal{V}$, are initialized to ∞ , except for $\psi_s = 0$. Furthermore, in **Algorithm 2**, the priority queue Q is used for storing the current leaves in the current search tree as well as their OF values in ψ , where the nodes in the priority queue Q are sorted in an ascending order based on the OF values. Specifically, the node with the minimum OF value has the top priority and thus will be first taken out. Moreover, $\text{prev}[v] = u$ indicates that the parent of node v is u and thus the route spanning from s to d can be constructed by visiting prev recursively. To speed up the search process over the solution space, we introduce an additional variable ψ_{\min} for storing the minimum delay spanning from the source node to the destination during the search process. Thus, ψ_{\min} provides an upper bound of the OF value, since problem (7) is a minimization problem of the total delay. The step in line 5 guarantees that ψ_{\min} is always the minimum OF value from s to d . Note that from the delay model of (6), the total delay spanning from the source node to any other node is monotonically increasing with the number of nodes in the route. As a consequence, the leaf node v in Q associated with $\psi_v > \psi_{\min}$ will be pruned as seen in line 8, which is capable of significantly reducing the search space, especially for large networks. However, in the worst-case scenario, **Algorithm 2** will have the same complexity as the standard Dijkstra algorithm [13], which is of the order of $\mathcal{O}(|\mathcal{E}| + |\mathcal{V}| \log |\mathcal{V}|)$.

V. SIMULATIONS

In this section, we evaluate the performance of the proposed algorithms by computer simulations. We first investigate the results based on simulations in Section V-A. Then we apply our algorithms to real flight datasets collected in the North-Atlantic region in Section V-B for validating the performance of the algorithms, which also reveals the potential benefits of AANETs in terms of improved connectivity.

A. Numerical Results

To model flight paths and the satellite orbits above the Earth surface, the spherical coordinate system denoted by (r, θ, φ) is considered, where the origin is located in the center of the earth. Furthermore, r is the distance of a point from the origin, while θ and φ are the polar angle and the azimuthal angle of the point, respectively. As a result, the locations of the ground BS, aircraft and satellites can be denoted

Algorithm 2: The shortest-path routing algorithm

Input : Weighted digraph of ANETs; The start node s and the destination d ;

Output: The optimal route R^* and the minimum delay ψ^* ;

Init. : A priority queue $Q = \emptyset$;

```

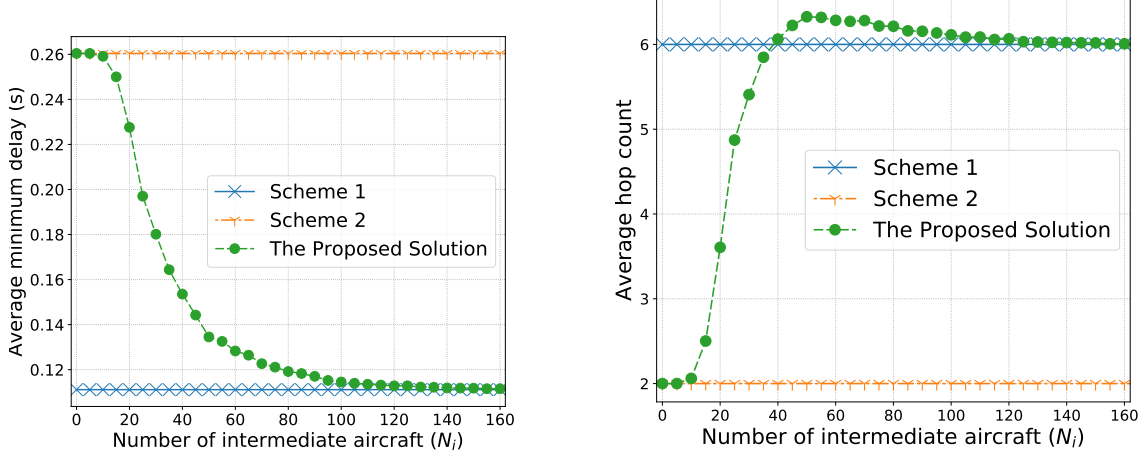
1 Initialize  $\psi = \{\psi_v, \forall v \in \mathcal{V}\}$ , where  $\psi_v = 0$  if  $v$  is  $s$ , and  $\psi_v = \text{inf}$  if otherwise. Set  $\psi_{min} = \text{inf}$ ;
2 Push  $\psi_s$  and  $s$  to  $Q$ ;
3 while  $Q$  is not empty do
4   Pop the vertex  $u$  and  $\phi_u$ ;
5   if  $u = d$  then
6      $\phi_{min} = \min\{\phi_{min}, \phi_u\}$ ;
7   while  $v$  is a neighbor of  $u$  do
8      $\hat{\psi} = \psi_u + D[e_{u,v}]$ ;
9     if  $\psi_v \geq \hat{\psi}$  and  $\psi_v \leq \psi_{min}$  then
10       $\psi_v = \hat{\psi}$ ;  $\text{prev}[v] = u$ ;
11      Store  $\psi_v$  and  $v$  into the  $Q$ ;
12 Constitute  $R$  from  $\text{prev}$ ;  $\psi^* = \psi_d$  and  $R^* = R$ ;
```

as $(r_g, \theta_g, \varphi_g)$, $(r_a, \theta_a, \varphi_a)$ and $(r_s, \theta_s, \varphi_s)$, respectively, where $r_i = H_i + r_{\text{earth}}$ for any $i \in \mathcal{N}$. To characterise the proposed algorithm, we first consider the simple scenario of $N_g = N_s = 1$. Specifically, $\theta_g = \varphi_g = 0$, which indicates that we treat the ground BS as the reference point of the system in the spherical coordinate system. The target aircraft is located at the point $\theta_d = \frac{\pi}{4}$ and $\varphi_d = \frac{\pi}{6}$, while the GEO satellite is located at the center of the region with $\theta_s = \frac{\pi}{8}$ and $\varphi_s = \frac{\pi}{12}$. Furthermore, the values of θ_a and φ_a for the intermediate aircraft are randomly drawn from a uniform distribution with $\theta_a \in [0, \theta_d]$ and $\varphi_a \in [0, \varphi_d]$, respectively. Hence, all figures are plotted over 1000 realizations. Note that the distance between the ground BS and the target aircraft is about 3300 km, and thus the ground BS cannot communicate directly with the target aircraft due to the curvature of the Earth. Moreover, we assume that the system operates at the mm-Wave frequency of $f_c = 31$ GHz and the noise power is $\sigma^2 = -132$ dBm [10]. The other parameters used in our simulations are the same as those in [12]. Specifically, the transmit powers of the ground BS, of the aircraft and of the satellite are 45dBm, 30dBm and 50dBm, respectively. Furthermore, we have $G_i^t = G_i^r = 25$ dB for the ground BS and the aircraft, while $G_i^t = G_i^r = 45$ dB for the satellite along with $B = 200$ MHz and $\phi_0 = 0$ dB. The heights of the ground BS, the aircraft as well as the satellite are 50m, 10.7 km and 35768 km, respectively. In particular, the greatest

distance between two points i and j above the horizon is calculated by $d_{vis} < 3.57(\sqrt{H_i} + \sqrt{H_j})$, where d_{vis} is in kilometers and H_i and H_j are in meters.

Fig. 2 illustrates the total delay and the number of hops in the shortest path¹ versus the number of intermediate relaying aircraft with different schemes, where the transport block size of $L = 9000$ bits is used as in [14]. For comparisons, we consider two different schemes. In Scheme 1, we assume that the ground BS is able to communicate with the target aircraft via A2AC links, which provides a lower bound of the end-to-end delay. Note that the distance between the ground BS and the target aircraft is around 3300 km in the model considered, hence it requires six hops at least due to the constraint of the visible distance. As a result, the lowest possible delay can be attained according to (6). In Scheme 2, we consider satellite aided communications, which only has two hops due to the large coverage area of the GEO satellite. Therefore, Fig. 2(a) illustrates how the total delay and the number of hops in the shortest path vary upon increasing the number N_i of intermediate aircraft. As seen from Fig. 2(a), the total delay of the proposed solution is substantially reduced upon increasing the number of intermediate aircraft. In particular, the minimum delay attained by the proposed algorithm closely approaches the lower bound of Scheme 1, when $N_i \geq 120$. This indicates that aircraft aided multi-hop communications substantially reduces the end-to-end delay upon using the proposed algorithm. As observed from Fig. 2(b), the hop count of the proposed solution is lower than that of Scheme 1 when $N_i < 35$ owing to occasionally opting for the satellite link as part of the shortest path for avoiding any potential route breakage. However, the hop count becomes higher than that of Scheme 1 when $N_i \leq 40$. Furthermore, the hop count of the proposed solution closely approaches that of Scheme 1 when $N_i \leq 120$ as in Fig. 2(a), which implies that the hop count in the proposed solution approaches the minimum number of hops required, when the number of intermediate aircraft is high enough. Fig. 3 illustrates the impact of the file size on the total delay. As seen from Fig. 3, the total delay between the source on the ground and the target aircraft is reduced upon increasing the number of aircraft, because this improves the probability of selecting a lower-delay aircraft-aided multi-hop link instead of the two-hop, yet high-delay satellite link for reaching the target aircraft. Therefore, when there is a shortage of intermediate aircraft, the ground BS communicates with the target aircraft via the satellite, which results in a higher propagation delay compared to A2AC links. In this context, the total propagation delay is dominated by that of the satellite links. Hence the delay versus N_i curve of Fig. 3 remains relatively flat when the number of aircraft is below about 20. Furthermore, we can observe that upon increasing the file size of L from 1Mbit to

¹Note that in this paper the number of hops in a path denotes the number of edges nodes in the path. For instance, consider a route with four nodes like $s \rightarrow n_1 \rightarrow n_2 \rightarrow d$, the number of hops is 3.



(a) Delay versus the number of the intermediate aircraft. (b) Hop counts versus the number of the intermediate aircraft.

Fig. 2. Comparisons of the total delay as well as the hop count for three different schemes.

9Mbit, the delay difference between $N_i = 0$ and $N_i = 100$ is substantially increased.

Let us elaborate briefly on a simple scenario with all links having an equal transmission rate of $C = 10\text{Mbps}$. For the satellite aided transmission, the total uplink and downlink propagation delay of the satellite is about $D_{pr} = 240\text{ms}$, while the total uplink plus downlink file-transfer delay is $D_{tr} = 40\text{ms}$ for a $L = 200\text{Kbit}$ file. Finally, the DF relaying delay is assumed to be $D_{df} = 20\text{ms}$. Thus, we can obtain the total delay of $D^{S2AC} = 300\text{ms}$ for an $L = 100\text{Kbit}$ file. By contrast, for the A2AC aided transmission relying on five hops in Scheme 1, the total propagation delay is around $D_{pr} = 11\text{ms}$ for a distance of 3300km , the file-transfer delay is $D_{tr} = 120\text{ms}$ and $D_{df} = 100\text{ms}$. Hence, we have the total delay of $D^{A2AC} = 231\text{ms}$. In this case, the A2AC aided transmission outperforms the satellite aided transmission. On the other hand, when the ground BS has an $L = 1\text{Mbit}$ file for transmission, we have $D^{S2AC} = 460\text{ms}$ while $D^{A2AC} = 711\text{ms}$, which results in a lower delay upon using the satellite than using the A2AC link². This reveals that aircraft aided multi-hop communications may have an advantage in providing lower-delay services than satellite aided communications, provided that the file is not excessively large.

B. Flight Data Driven Results

In this subsection, we characterize the system performance for the five busiest TransAtlantic airlines using real historical flight data collected over the North-Atlantic region, which includes Delta Airline, United Airline, American Airline, British Airways and Lufthansa. Specifically, these datasets contain the

²Note that given a transmission rate C , there is a threshold L_{th} , where the A2AC aided transmission is beneficial if $L < L_{th}$, otherwise the satellite aided transmission has a lower delay. In particular, from the delay model of (6), we have $L_{th} \approx \frac{3.658C}{100}$

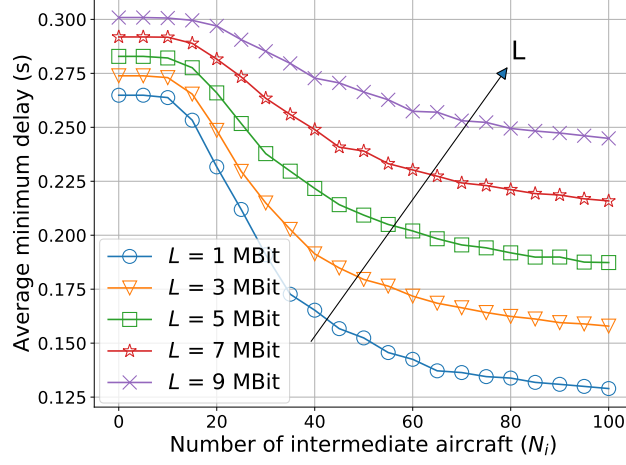


Fig. 3. The impact of file size on the minimum delay.

historical flight information of the area recorded at sampling intervals of 10s, where each entry of the flight contains the following information: timestamp, longitude, latitude, altitude and speed. The data in the first and second datasets are collected from 00:00 on 24 Dec. 2017 until 00:00 on 26 Dec. 2017, which is typically the quietest day of the year. The first dataset, referred to as Data-1, contains the TransAtlantic flights between LHR Airport and JFK Airport as in the previous example, which consists of 57 flights and 17,281 entries for each flight. The second dataset, referred as Data-2, contains all TransAtlantic flights of the 5 busiest TransAtlantic airlines, which consists of 381 flights and 17,281 entries for each flight. The data in the third dataset were collected from 00:00 on 29 Jun. 2018 to 00:00 on 30 Jun. 2018, which is the busiest day of the year having the most flights. Similar to the scenario of Data-2, the third dataset, Data-3, contains 649 flights and 8,641 entries for each flight. Moreover, the file size used is $L = 200\text{Kbit}$ and all the other parameters used in our simulations are the same as in Section V-A.

Fig. 4 shows an example topology of the AANET attained from Data-2 and Data-3 as well as the shortest paths found from the ground BS at LHR to BA117, when the flight distance of BA117 is 3532 km and each link has a fixed file-transfer rate $C = 10\text{Mbps}$. In Fig. 4, the stars denote LHR (the ground BS) and JFK, while green circles denote the planes in the network. Furthermore, the red dashed lines denote the shortest path to BA117 (the square) and the triangles are the intermediate planes. As seen from Fig. 4(a), the shortest path from the ground BS at LHR to BA117 in Data-2 has seven hops (Ground BS \rightarrow DL229 \rightarrow AA151 \rightarrow UA53 \rightarrow DL231 \rightarrow BA195 \rightarrow DL83 \rightarrow BA117) and its delay is 272.46ms, while the shortest path found for BA117 in Data-3 has six hops (GroundBS \rightarrow UA988 \rightarrow UA24 \rightarrow DL177 \rightarrow AA25 \rightarrow AA725 \rightarrow BA117) and its delay is 231.75ms in Fig. 4(b). We can see that both the delay and the hop count of the shortest path found for Data-3 is lower than that for Data-2, which confirms that the AANET has lower delay during the busiest day than that in the quietest day of the year. This is owing to the fact that there are

more flights in Data-3 than in Data-2, since having more planes available approaches the ideal scenario of Scheme 1.

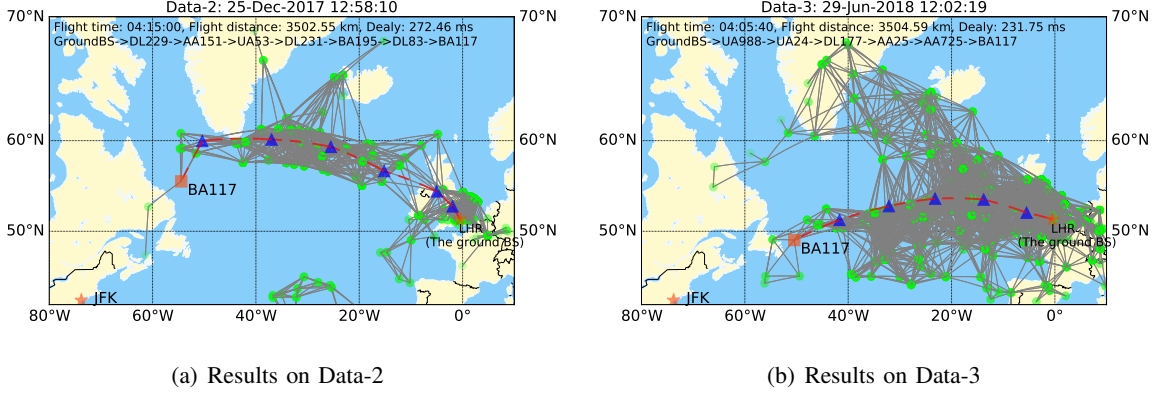


Fig. 4. Comparisons of BA117 in AANETs over different datasets.

Fig. 5 shows the cumulative degree distribution (CDD) of the connected graph modelling different networks generated from the three datasets for providing us with a glimpse into the structure of a network, where the CDD represents the specific fraction of nodes having a degree smaller than a given number k on the abscissa axis. We observe that there are many nodes with degree zero for Data-1, which implies that there is no communication link between the ground BS at LHR and BA117. Furthermore, we can see that the probability of the nodes with the degree of $k \geq 12$ is about 20% for Data-2, while it is higher than 40% for Data-3. Moreover, the maximum degree of a node in Fig. 5 for Data-3 is 276, while it is 160 for Data-2 and 12 for Data-1, respectively.

Fig. 6 shows the cumulative distribution functions (CDFs) of both the hop count and of the total delay of the shortest paths found during the period of the complete travel of BA117 from LHR to JFK. Explicitly, Fig. 6(a) and Fig. 6(b) shows the cumulative probability distributions of the hop count and the total delay in the shortest paths found in the three datasets throughout the complete travel of BA117. It can be observed from the delay model of (6) that the total delay of a route relies on the number of hops. As a result, the CDF curves of the hop count have the similar trends as those of the total delay in terms of the shortest paths found. Furthermore, Fig. 6 also illustrates that both the hop count and the delay attained from Data-3 are more beneficial than those of Data-2 and Data-1, since there are more available flights in Data-3. More specifically, observe from Fig. 6 that during the complete period of travel there is a low success probability of around 30% for BA117 to communicate with the ground BS via AANETs for Data-1. By contrast, for Data-2 and Data-3, BA117 is capable of connecting to the ground BS via multi-hop communications during its complete travel.

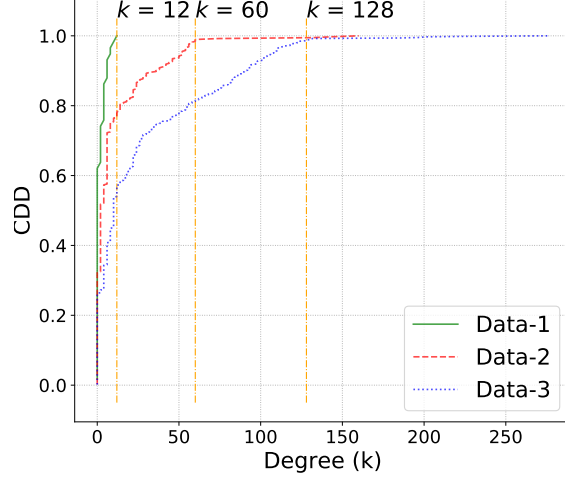


Fig. 5. Degree distribution of AANET with different datasets.

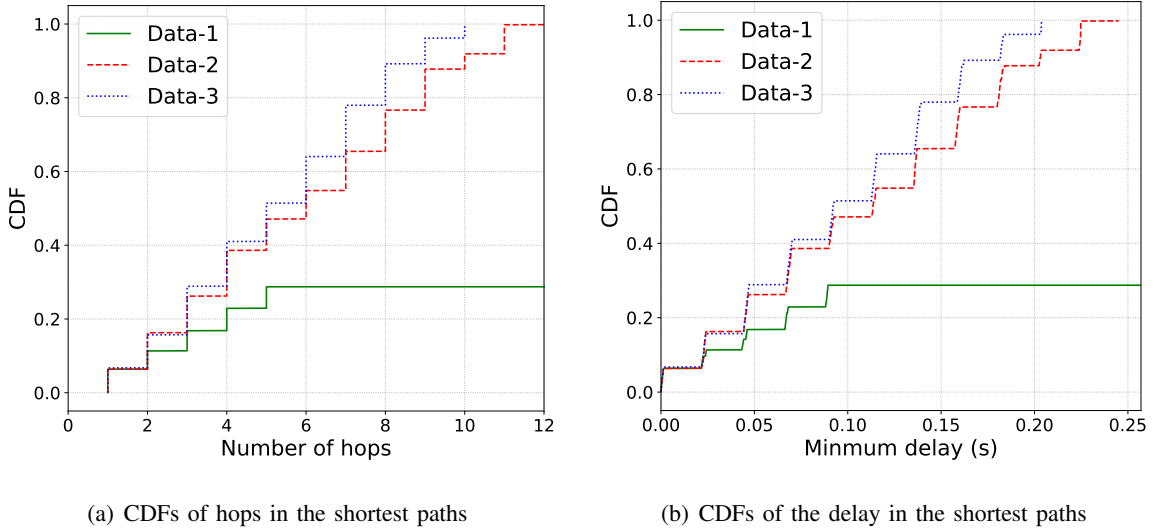


Fig. 6. CDFs of hops and the total delay of the shortest paths found by the proposed algorithm.

VI. CONCLUSIONS

In this paper, we investigated the routing problem of AANET-assisted integrated ground-air-space communications with the objective of providing in-flight connectivity. Whilst relying both on aircraft and ground BSs as well as satellites, we minimized the total delay by considering the propagation delay, file-transfer delay and DF relaying delay. Furthermore, we have developed a weighted digraph for modelling the integrated AANET under minimum-rate constraints for finding the optimal route. Both the simulation results and real historical flight data driven results revealed that the AANET-aided transmission has the potential benefit of extending the DA2GC coverage while providing reduced-delay transmissions. A promising extension of this research is to consider the multi-component Pareto-optimization of AANET-

assisted integrated networks for striking a compelling tradeoff amongst different performance metrics such as the delay, the energy efficiency as well as spectral efficiency, just to name a few.

REFERENCES

- [1] (2019) Global Market Forecast. [Online]. Available: <https://www.airbus.com/aircraft/market/global-market-forecast.html>
- [2] M. Vondra, E. Dinc, M. Prytz, M. Frodigh, D. Schupke, M. Nilson, S. Hofmann, and C. Cavdar, "Performance study on seamless DA2GC for aircraft passengers toward 5G," *IEEE Commun. Mag.*, vol. 55, no. 11, pp. 194–201, Nov. 2017.
- [3] J. Zhang, T. Chen, S. Zhong, J. Wang, W. Zhang, X. Zuo, R. G. Maunder, and L. Hanzo, "Aeronautical *ad hoc* networking for the Internet-above-the-clouds," *Proc. IEEE*, vol. 107, no. 5, pp. 868–911, May 2019.
- [4] Gogo-blog. (2019) Gogo Reaches Approximately 1,300 Commercial Aircraft Installed with Satellite IFC Technology. [Online]. Available: <https://concourse.gogoair.com/>
- [5] (2015, Sep.) The European aviation network. [Online]. Available: <https://www.telekom.com/resource/blob/390304/.../dl-150929-datenblatt-data.pdf>
- [6] D. Rieth, C. Heller, and G. Ascheid, "Aircraft to ground-station C-band channel—small airport scenario," *IEEE Trans. Veh. Technol.*, vol. 68, no. 5, pp. 4306–4315, 2019.
- [7] S. Fu, J. Gao, and L. Zhao, "Integrated resource management for terrestrial-satellite systems," *IEEE Trans. Veh. Technol.*, vol. 69, no. 3, pp. 3256–3266, 2020.
- [8] E. W. Dijkstra, "A note on two problems in connexion with graphs," *Numerische Mathematik*, vol. 1, no. 1, pp. 269–271, Dec 1959. [Online]. Available: <https://doi.org/10.1007/BF01386390>
- [9] T. Z. H. Ernest, A. S. Madhukumar, R. P. Sirigina, and A. K. Krishna, "Outage analysis and finite SNR diversity-multiplexing tradeoff of hybrid-duplex systems for aeronautical communications," *IEEE Trans. Wireless Commun.*, vol. 18, no. 4, pp. 2299–2313, Apr. 2019.
- [10] S. Hofmann, A. E. Garcia, D. Schupke, H. E. Gonzalez, and F. H. Fitzek, "Connectivity in the air: Throughput analysis of air-to-ground systems," in *IEEE Proc. of International Commun. Conf. (ICC)*, May 2019, pp. 1–8.
- [11] T. Cuvelier and R. W. Heath, "Mmwave MU-MIMO for aerial networks," in *Int. Symp. Wireless Commun. Sys. (ISWCS)*, Aug. 2018, pp. 1–6.
- [12] M. Vondra, M. Ozger, D. Schupke, and C. Cavdar, "Integration of satellite and aerial communications for heterogeneous flying vehicles," *IEEE Network*, vol. 32, no. 5, pp. 62–69, Sep. 2018.
- [13] M. L. Fredman and R. E. Tarjan, "Fibonacci heaps and their uses in improved network optimization algorithms," *J. ACM*, vol. 34, no. 3, p. 596–615, Jul. 1987. [Online]. Available: <https://doi.org/10.1145/28869.28874>
- [14] 3GPP, "5G NR: Packet Data Convergence Protocol (PDCP) specification," *3GPP TS 38.323*, vol. version 15.2.0 Release 15, Sep. 2018.